Supporting Information

Impact of Synthetic Route on Structural and Physical Properties of Butyl-1,4-Diammonium Lead Iodide Semiconductors

Majid Safdari[a], Dibya Phuyal[b], Bertrand Philippe[b], Per H Svensson[a,e], Sergei Butorin[b], Kristina Kvashnina[c,d], Håkan Rensmo[b], Lars Kloo[a] and James M. Gardner[a*]

[a]Applied Physical Chemistry, Department of Chemistry, KTH Royal Institute of Technology, SE-100 44, Stockholm, Sweden.

[b]Dept. of Physics and Astronomy, Uppsala Univ., Box 516, SE-75121, Uppsala, Sweden

[c]ESRF- The European Synchrotron, CS40220, 38043 Grenoble Cedex 9, France

[d]Helmholtz Zentrum Dresden-Rossendorf, Institute of Resource Ecology, 01314 Dresden, Germany

[e]SP Process Development, Forskargatan, 15121 Södertälje, Sweden

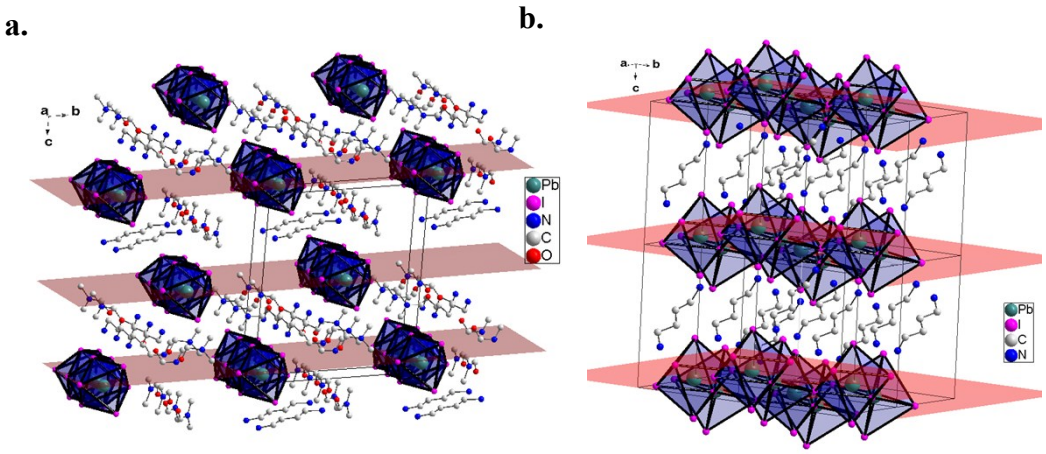

Figure S1. Comparable connectivity of PbI_6 octahedral units along the 001 structural planes in a. $(BdA)Pb_2I_6$ b. $(BdA)PbI_4$.

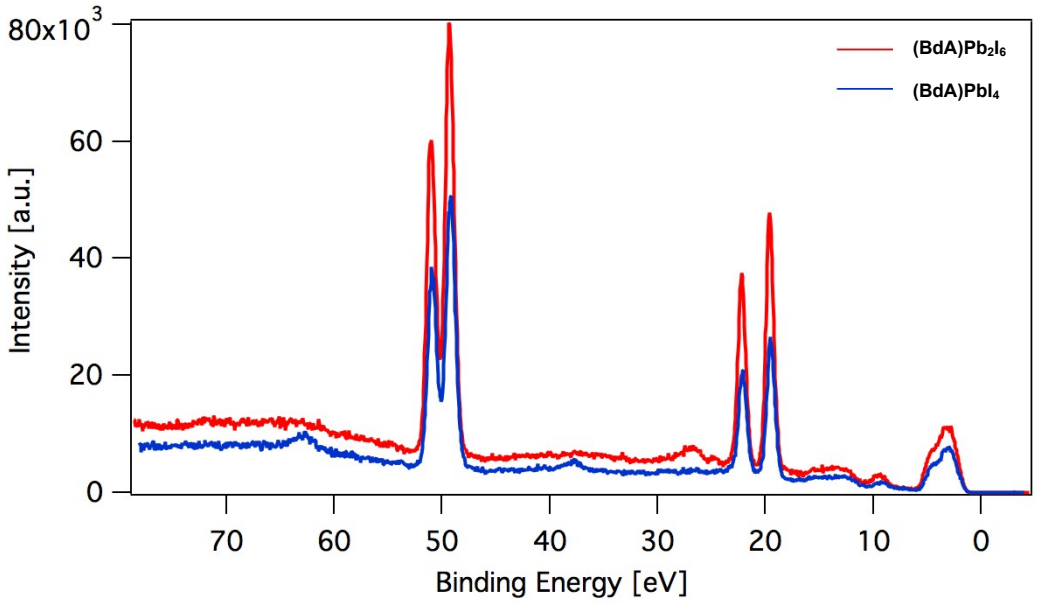

Figure S2. Extended Valence Band spectra recorded at 4000 eV photon energy for --- $(BdA)Pb_2I_6$ and --- $(BdA)PbI_4$. These spectra were used to calculate iodide/lead ratios.

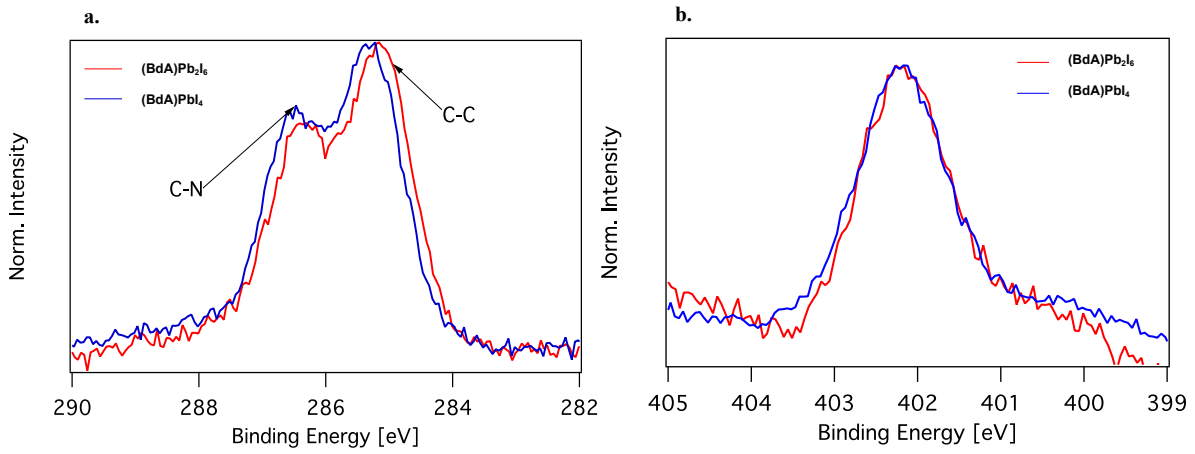

Figure S3. XPS spectra of a. carbon, and b. nitrogen for --- $(BdA)Pb_2I_6$ and --- $(BdA)PbI_4$. Two peaks were recorded for carbon that originate from two types of carbons in both products while only a single nitrogen was observed.

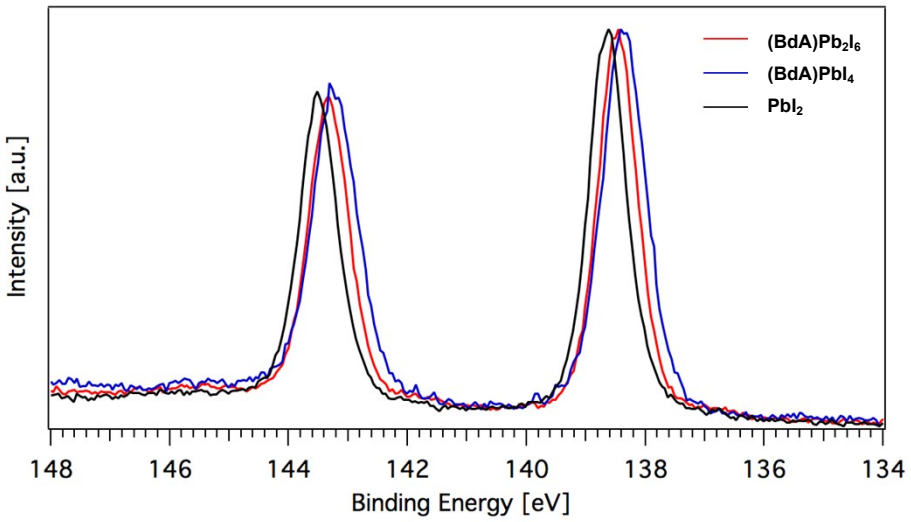

Figure S4. Hard X-Ray XPS spectra of Pb 4*f* for --- $(BdA)Pb_2I_6$ and --- $(BdA)PbI_4$. There is a small metallic component of Pb^0 around 137.0 eV. The difference between $(BdA)Pb_2I_6$ and $(BdA)PbI_4$ is approximately 0.05 eV.

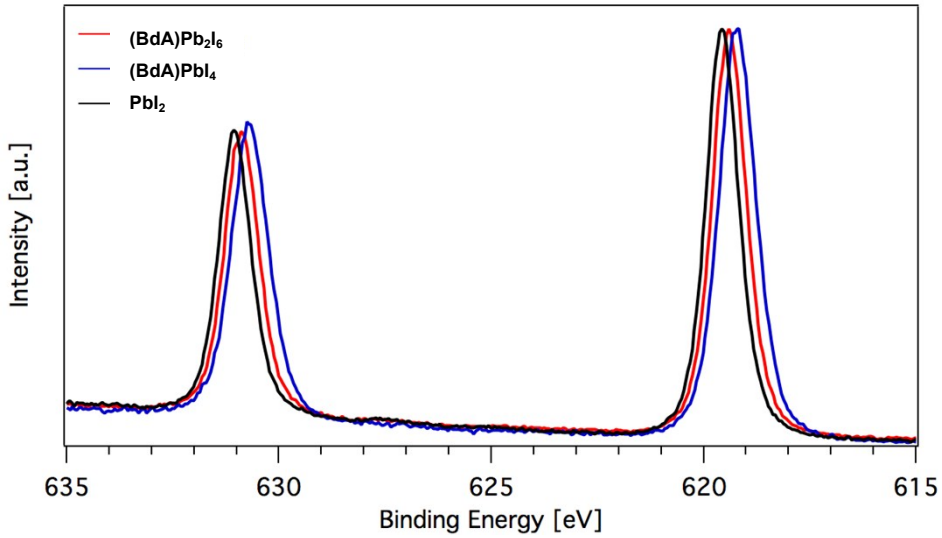

Figure S5. Hard X-Ray XPS spectra of I 3*d* for --- $(BdA)Pb_2I_6$ and --- $(BdA)PbI_4$.

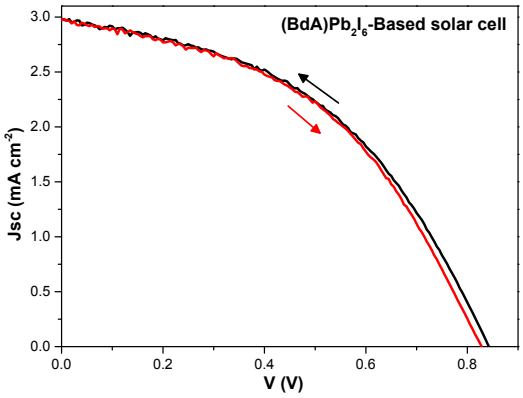

	η (%)	Voc (V)	Jsc ($mAcm^{-2}$)	FF
Forward	**1.13**	**0.845**	**2.98**	**0.450**
Reverse	**1.12**	**0.830**	**2.97**	**0.453**

Figure S6. IV hysteresis for the $(BdA)Pb_2I_6$ solar cells at scan rate of 10 mV/s for bias voltage.

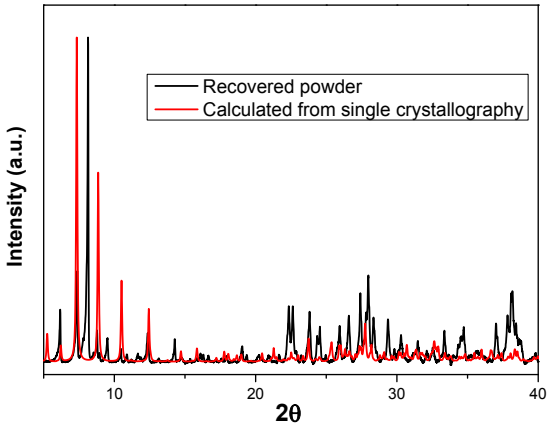

Figure S7. Comparison of XRD powder diffraction pattern of [---] solvated and [---] non-solvated $(BdA)Pb_2I_6$.

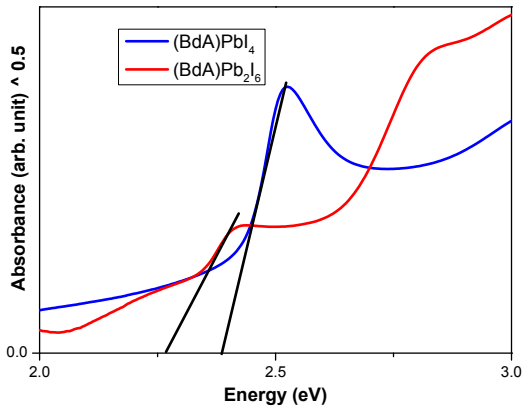

Figure S8. Tauc plot of --- $(BdA)Pb_2I_6$ and --- $(BdA)PbI_4$.

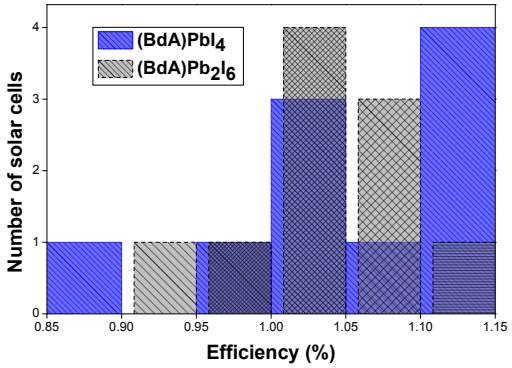

Figute S9. Histogram for the variations of the solar cell's efficiencies for 10 fabricated solar cells based on $(BdA)Pb_2I_6$ and $(BdA)PbI_4$ light absorber.

Table S1. IV characteristics of 10 fabricated solar cells based on $(BdA)PbI_4$ light absorber.

#Device based on $(BdA)PbI_4$	η (%)	Voc (V)	Jsc (mA cm^{-2})	FF
1	1.001	0.91	2.56	0.43
2	0.961	0.88	2.32	0.471
3	0.899	0.87	2.067	0.5
4	1.102	0.905	2.932	0.415
5	1.045	0.88	2.63	0.451
6	1.12	0.93	2.738	0.44
7	1.094	0.92	2.666	0.446
8	1.146	0.925	2.733	0.453
9	1.114	0.915	3.022	0.403
10	1.044	0.905	3.075	0.375
Average	1.053	0.904	2.674	0.438
STDEV	0.079	0.021	0.310	0.035

Table S2. IV characteristics of 10 fabricated solar cells based on $(BdA)Pb_2I_6$ light absorber.

#Device based on $(BdA)Pb_2I_6$	η (%)	Voc (V)	Jsc (mA cm^{-2})	FF
1	1.087	0.855	2.733	0.465
2	1.144	0.85	2.906	0.463
3	1.045	0.81	2.961	0.436
4	1.051	0.825	2.743	0.465
5	0.997	0.795	3.084	0.406
6	1.025	0.795	2.82	0.457
7	0.94	0.76	2.826	0.438
8	1.045	0.81	2.961	0.436
9	1.051	0.825	2.743	0.46
10	1.03	0.805	2.934	0.436
Average	1.042	0.813	2.871	0.446
STDEV	0.053	0.028	0.117	0.019